Geotechnical and Geological Engineering (2006) 24: 1089–1102
DOI 10.1007/s10706-005-7464-x

Technical Note

Visualization of rock mass classification systems

MING CAI* and PETER KAISER
Geomechanics Research Centre, MIRARCO, Laurentian University, Sudbury, Ontario, Canada

(Received 7 September 2004; accepted 16 May 2005)

Abstract. A rock mass classification system is intended to classify and characterize the rock masses, provide a basis for estimating deformation and strength properties, supply quantitative data for mine support estimation, and present a platform for communication between exploration, design and construction groups. In most widely used rock mass classification systems, such as *RMR* and *Q* systems, up to six parameters are employed to classify the rock mass. Visualization of rock mass classification systems in multi-dimensional spaces is explored to assist engineers in identifying major controlling parameters in these rock mass classification systems. Different visualization methods are used to visualize the most widely used rock mass classification systems. The study reveals that all major rock mass classification systems tackle essentially two dominant factors in their scheme, i.e., block size and joint surface condition. Other sub-parameters, such as joint set number, joint space, joint surface roughness, alteration, etc., control these two dominant factors. A series two-dimensional, three-dimensional, and multi-dimensional visualizations are created for *RMR*, *Q*, Rock Mass index *RMi* and Geological Strength Index (*GSI*) systems using different techniques. In this manner, valuable insight into these rock mass classification systems is gained.

Key words. block volume, joint, jointed rock mass, multi-dimension, rock classification, visualization.

1. Introduction

Human beings are overpoweringly visual creatures. As shown in Figure 1, visual sight constitutes 70% of sense to object perception. When combined with sound, it completes 90% of our perception to objects. Visualization is here defined as the process of exploring, transforming, and viewing data as images to gain understanding and insight into data. It is a part of our everyday life. Visualization is the task of generating images that allow important features in the data to be recognized much more readily than from processing raw data by other means, for example, statistics. It makes the best use of our highly developed visual senses which are capable of detecting complex and subtle patterns in images. Visualization also enables the identification of data features that are otherwise hidden or difficult to grasp.

For three- or four-dimensional data visualization, the dimensions are not well understood if the graph is not in stereo or color. That is why virtual reality (VR)

* Corresponding author: Geomechanics Research Centre, MIRARCO, Laurentian University, Sudbury, Ontario, Canada. e-mail: mcai@mirarco.org

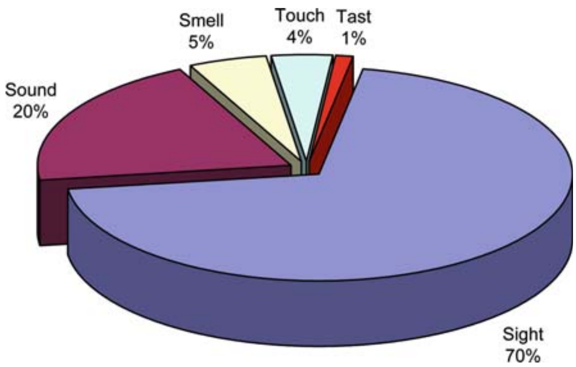

Figure 1. Relative importance of senses to object perception (Schroeder 1996).

visualization technique becomes very effective when viewing complex multi-dimensional dataset. The power of VR lies in the ability to visualize information and make decisions based on what is seen, without going through elaborate mathematics or expensive trial and error processes. VR has opened a way to process data as a 'visual scientist.' For most of us, with our way of thinking and the way in which we experience the world, it is difficult to imagine more than three spatial dimensions. A full stress tensor, for example, has six dimensions and its visualization is vital for the interpretation of results from 3D stress models. Jeremie et al. (2002) discussed different approaches, such as hedgehogs, hyperstreamlines, hyperstreamsurfaces, isosurfaces, for stress tensor visualization in computational geomechanics. Another example is the application of visualization technique to assist better understanding the complex constitutive models in material science. The simplest constitutive model have one independent parameter but some complex models may have over one dozen independent parameters or dimensions. Hashash et al. (2002) developed a visual framework for the visualization of constitutive models. The mathematical equations and matrix quantities describing the constitutive models are represented by multi-dimensional geometric/visual objects to assist the easy use and understanding of these models.

In rock mechanics, many rock mass classification systems, such as Q (Barton et al., 1974), RMR (Bieniawski, 1973), Geological Strength Index (GSI) (Hoek et al., 1995) systems, have been proposed and used. Because there are many controlling factors or dimensions in the rock mass classification systems, it is often difficult for inexperienced users to understand the importance of each factor and its influence on the classification index. Furthermore, developers of new rock mass classification systems need to have a comprehensive understanding of previous systems before starting their own development. Bearing in mind the powerful visual sense we possess, it seems evident that our understanding of the existing rock mass classification systems and the underlying connection between the systems can be improved if properly visualized.

This paper describes a framework for transforming the representation of rock mass classification systems from a series of mathematical equations and table quantities to multi-dimensional geometric/visual objects using different techniques. The present results provide a mental framework for engineers and students to better understand the widely used rock mass classification systems and the implied rock mass conditions.

2. Rock mass classification systems

2.1. RMR SYSTEM

This rating system was proposed by Bieniawski (1973, 1976, 1989) for use in design of tunnels in hard and soft rock. A revision was made in 1989 to reflect more data collected. Six parameters are used to classify a rock mass using the *RMR* system, that is,

- Uniaxial compressive strength of rock material (A1)
- Rock Quality Designation (*RQD*) (A2)
- Joint spacing (A3)
- Joint condition (A4)
- Groundwater condition (A5)
- Joint orientation (A6). The final rating is the summation of all ratings for the six parameters, that is,

$$RMR = A1 + A2 + A3 + A4 + A5 + A6 \tag{1}$$

RMR value ranges from 0 to 100. Details of the rating for each parameter are presented as tables (Bieniawski, 1989) and are not repeated here.

2.2. Q SYSTEM

The *Q*-system, developed by Barton et al. (1974), was based on the study of over 200 tunnels and used for the determination of rock mass characteristics and tunnel support requirements. Six parameters are chosen to define *Q* as

$$Q = \frac{RQD}{J_n} \cdot \frac{J_r}{J_a} \cdot \frac{J_w}{SRF} \tag{2}$$

where *RQD* is the Rock Quality Designation, J_n is the joint set number, J_r is the joint roughness number, J_a is the joint alteration number, J_w is the joint water reduction factor and *SRF* is the stress reduction factor. The rating for each parameter (except for *RQD*) is also presented in tables (Barton et al., 1974). For mining application, dry conditions are often assumed and the stress is considered by separate stress modeling so that the modified rock quality index for mining is defined as

$$Q\prime = \frac{RQD}{J_n}\frac{J_r}{J_a} \tag{3}$$

Q or *Q′* values for most rock masses range from 0.001 to 1000.

2.3. RMI SYSTEM

The Rock Mass index (*RMi*) was developed to characterize the strength of the rock mass for construction purpose (Palmstrøm, 1996a, b). *RMi* is based on the reduced rock strength caused by jointing and is expressed as

$$RMi = 0.2\sigma_c\sqrt{jC} \cdot V_b^{0.37jC^{-0.2}} \tag{4}$$

where σ_c is the uniaxial compressive strength of intact rock measured on 50 mm samples and V_b is the block volume given in cubic meters and *jC* is the joint condition factor expressed as

$$jC = jL\frac{jR}{jA} \tag{5}$$

where *jL*, *jR* and *jA* are factors for joint length and continuity, joint wall roughness, and joint surface alteration, respectively. Ratings for the factors *jR*, *jA* and *jL* are given in tables (Palmstrøm, 1996a). Values of *RMi* range from 0 to σ_c.

2.4. GSI SYSTEM

To provide a practical means to estimate the strength and deformation modulus of jointed rock masses for use with the Hoek-Brown failure criterion (Hoek and Brown 1980, 1988, 1997; Hoek et al. 2002), the *GSI* was introduced (Hoek et al., 1995). The value of *GSI* ranges from 0 to 100. The *GSI* system consolidates various versions of the Hoek–Brown criterion into a single simplified and generalized criterion that covers all of the rock types normally encountered in underground engineering. A *GSI* value is determined from the structure interlocking and joint surface conditions shown in a table. The early version of the *GSI* system was presented as a table (Hoek et al., 1995) and a revised version was presented as a chart (Hoek and Brown, 1997). For good quality rocks, *GSI* value and *RMR* value are comparable.

3. Visualization in two-dimensional space

It is seen that the widely used rock mass classification systems contain multiple influencing parameters or dimensions. For example, *RMR* system has six parameters. *RMi* system has three explicit parameters (Equation (4)) and if the implicit parameters (Equation (5)) are included, there are five independent parameters in total. To begin with, we make some simplifications about the parameters, that is, parameters are grouped into categories. The simplest way to present visual representation of the rock mass classification systems is to reduce the dimensions to two because a two-dimensional function $f=f(x_1,x_2)$ can be viewed as a surface. In the following discussion, we condense some parameters into one category and reduce the total parameters in a rock mass classification system to two for visualization in a two-dimensional space. One logical way to do this is to group the parameters into one group that describes the rock or block volume and another group that describes the joint conditions.

3.1. RMR SYSTEM

In the *RMR* system, factors A1, A2 and A3 describe the size and competence of the rock mass, while factors A4 and A5 defines the joint condition. Ignoring A6, the joint orientation modification factor, we can represent the *RMR* index as a two-dimensional function as

$$RMR = \underbrace{A1 + A2 + A3}_{x_2} + \underbrace{A4 + A5}_{x_1} \tag{6}$$

According to the rating in the *RMR* system, x_1 and x_2 vary between 0–45 and 0–55, respectively. In the original system, the rating for each parameter is given in tables as lump or step ratings. However, as suggested by Sen and Sadagah (2003), continuous representation of the rating is possible. The *RMR* function shown in Equation (6) is plotted in Figure 2 assuming continuous variation/rating for each parameter. This figure illustrates that *RMR* is simply a planar representation of the rock mass quality in this two-dimensional visualization. The contours on the bottom are vertical projections of the contours of the inclined surface.

3.2. Q SYSTEM

In the two-dimensional representation of the *Q*' index, we consider the first dimension as $\frac{Jr}{Ja}$ (inter-block shear strength) and the second dimension as $\frac{RQD}{j_n}$ (block size). Thus, we can represent the *Q*' index as a two-dimensional function as

$$Q\prime = \underbrace{\left(\frac{RQD}{J_n}\right)}_{x_2} \cdot \underbrace{\left(\frac{J_r}{J_a}\right)}_{x_1} \tag{7}$$

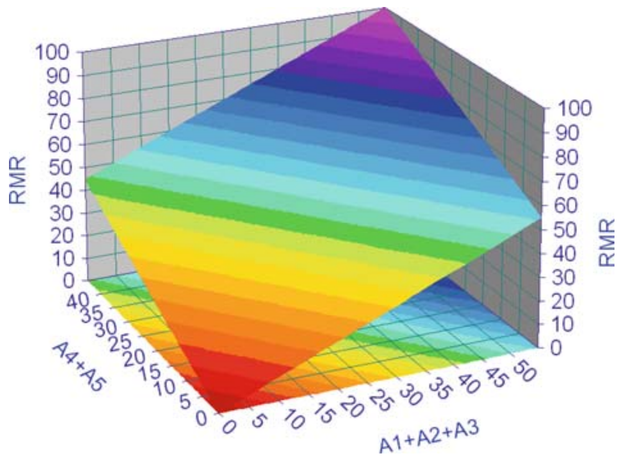

Figure 2. *RMR* system visualized in two-dimensional space.

According to the Q system, x_1 and x_2 vary between 0.02–5.33 and 0–200, respectively. In a log–log–log plot, and assuming continuous variation of each parameter, Q' is also represented by a plane as shown in Figure 3.

This visualization shows incredibly that the RMR and Q system eventually represent rock mass in the same manner, one in a linear and the other in a log space.

3.3. RMI SYSTEM

RMi system is visualized with two parameters jC and V_b from the following function

$$RMi = 0.2\sigma_c\sqrt{jC}\cdot V_b^{0.37jC^{-0.2}}, \quad jC \to x_1, \quad V_b \to x_2 \tag{8}$$

where σ_c is kept as a constant. According to the RMi system, jC vary from 0.015 to 72. The function is plotted in Figure 4 for $\sigma_c = 100$ MPa. With very large block volume and high jC value, the function gives an RMi value which is greater than σ_c, which is physically impossible. Therefore, an upper bound limit of $RMi \le \sigma_c$ should be considered (Figure 4). In a log–log–log plot, the RMi is a surface very close to a plane. Because the exponential jC, the RMi surface is not a planner.

3.4. GSI SYSTEM

To facilitate the easy use of the GSI system, Cai et al. (2004) proposed a quantitative approach for the GSI chart. It employs the block volume (V_b) and a joint condition factor (J_c) as quantitative characterization factors. The approach is built on the linkage between descriptive geological terms and measurable field parameters such as joint spacing and joint roughness. The newly developed approach adds quantitative means to facilitate the use of the system, especially by inexperienced engineers.

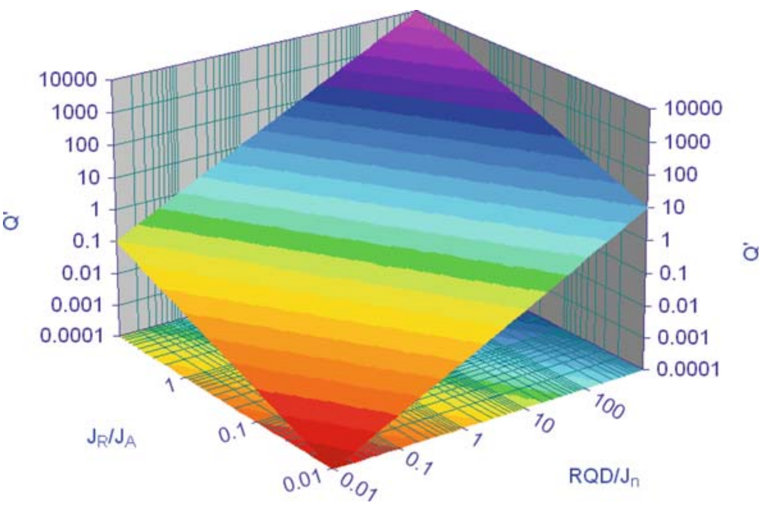

Figure 3. Q' system visualized in two-dimensional space.

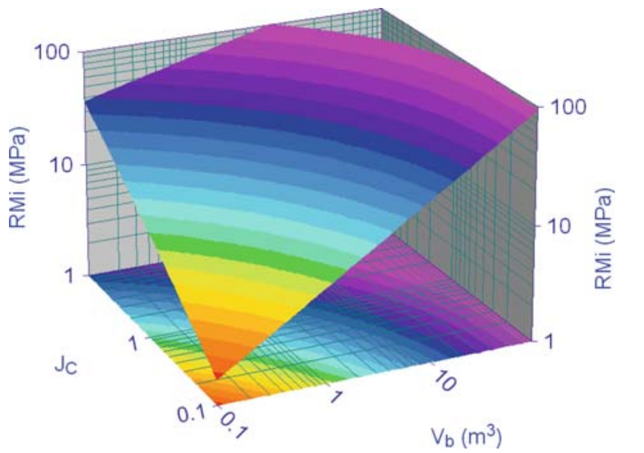

Figure 4. RMi system visualized in two-dimensional for $\sigma_c = 100$ MPa, with $RMi \le \sigma_c$ cut-off.

Based on the proposed quantitative chart, and using surface fitting techniques, the relationship between GSI and J_c and V_b is found to be

$$GSI = \frac{26.5 + 8.79 \ln J_c + 0.9 \ln V_b}{1 + 0.0151 \ln J_c - 0.0253 \ln V_b}, \quad J_c \to x_1, \quad V_b \to x_2 \tag{9}$$

where J_c is a dimensionless factor and V_b is in cubic centimeters. Equation (9) provides a convenient way to utilize the GSI system in computer codes, eliminating the need to refer to the GSI chart. The user needs only to supply the block volume and joint condition factor to calculate the GSI value and hence the Hoek–Brown strength parameters and deformation modulus of the jointed rock mass. In other words, the Hoek–Brown strength parameters and deformation modulus can be directly expressed as a function of V_b and J_c. In a log–log plot (Figure 5), the GSI is a surface which is very close to a plane, with $x_1 = J_c$ as and $x_2 = V_b$.

3.5. DISCUSSION

RMR, Q, RMi and GSI systems have been visualized in two-dimensional space by condensing classification parameters into one that governs the block volume and the other that governs the joint surface condition. The plots from Figures 2 to 5 reveal one common feature of these widely used rock mass classification systems, that is, the most important controlling factors are block volume and joint surface condition. When parameters are condensed to only these two parameters, the classification functions are best represented by planar surfaces in linear (RMR) or log scales (Q), or by surfaces that are very close to planar surfaces in log scales (GSI and RMi). RMR is a planner in linear scale and Q is also a planner in log scale. GSI and RMi show some nonlinearity but the surfaces are comparable to planners. Thus, it can be concluded that all the rock mass classification systems are essentially the same. The relative contribution of these two controlling parameters is easily seen from these

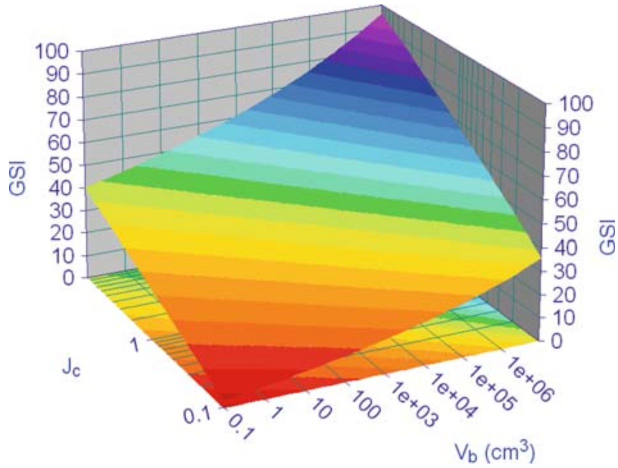

Figure 5. Two-dimensional *GSI* system visualization.

visual plots. Larger block volume and better joint surface conditions lead to a higher classification index. It is concluded that any new development of rock mass classification system should therefore start with careful consideration of the block size and joint surface condition characterization. From this simple exercise, we find that visualization of the rock mass classification systems does help us gain a deeper understanding of the systems and the underlying controlling parameters.

4. Visualization in three-dimensional space

When there are three parameters or when multi-parameters are condensed to three parameters in a rock mass classification system, that is,

$$f = f(x_1, x_2, x_3) \tag{10}$$

the best way to visualize the system is to represent $f(x_1, x_2, x_3)$ by using iso-surfaces.

4.1. RMR SYSTEM

When the parameters A1–A3 are condensed into one that represents the rock block size and competence, and A4 (joint condition) and A5 (ground water condition) are treated independently, the *RMR* system function can be rewritten as

$$RMR = \underbrace{A1 + A2 + A3}_{x_2} + \underbrace{A4}_{x_1} + \underbrace{A5}_{x_5} \tag{11}$$

The *RMR* system with three condensed parameters is illustrated in Figure 6 using a series of iso-surfaces. The linear influence of each parameter on the *RMR* value can be clearly detected. Alternatively, one can populate a voxet with data and use a slider to move in x_1, x_2, x_3 directions in an interactive manner to reveal the influence of each parameter on the *RMR* value.

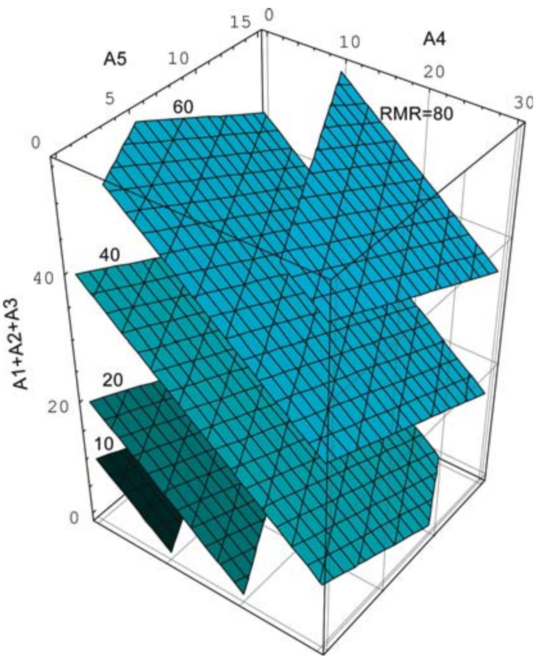

Figure 6. Three-dimensional contours of *RMR* (80, 60, 40, 20, 10).

4.2. RMI SYSTEM

Similarly, the *RMi* system is visualized considering σ_c, jC and V_b as three independent parameters, that is,

$$RMi = 0.2\sigma_c\sqrt{jC} \cdot V_b^{0.37jC^{-0.2}}, \quad \sigma_c \to x_1, \ \ jC \to x_2, \ \ V_b \to x_3 \tag{12}$$

The contours representing $RMi = 100, 50, 25$ are presented in Figure 7, with V_b axis being in log scale. This visualization best fits the expression originally provided by Equation (12).

4.3. GSI SYSTEM

We consider the two influence factors, joint roughness and alteration, for the joint condition factor and rewrite Equation (9) as

$$GSI = \frac{26.5 + 8.79\ln\frac{J_R}{J_A} + 0.9\ln V_b}{1 + 0.0151\ln\frac{J_R}{J_A} - 0.0253\ln V_b}, \quad J_R \to x_1, \ \ J_A \to x-2, V_b \to x_3 \tag{13}$$

where J_R (joint roughness number), J_A (joint alteration number) and V_b have been considered as independent parameters. The contours representing $GSI = 80, 60, 40, 20, 10$ are presented in Figure 8, with V_b axis being in log scale. The influence of joint

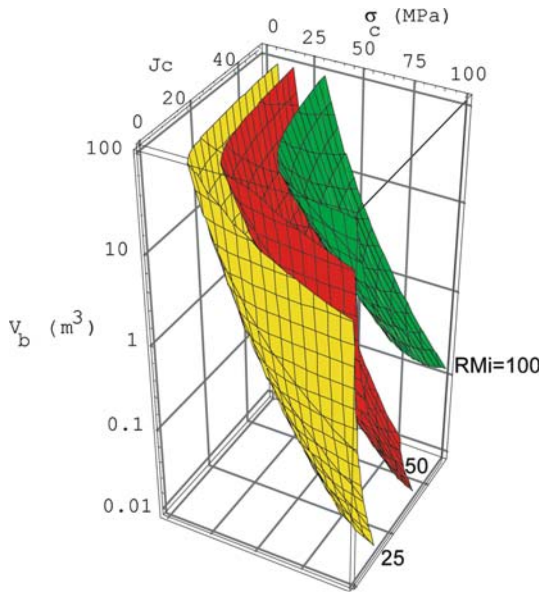

Figure 7. Three-dimensional contours of *RMi* (green: $RMi = 100$, red: $RMi = 50$, blue: $RMi = 25$). V_b axis is in log scale.

roughness and alteration can be examined using these plots. Again, the large influence of V_b on the *GSI* value can be seen from these plots.

Three-dimensional representation of functions of a rock mass classification system with three parameters is best achieved by a voxet using iso-surfaces or sliders in an interactive environment. The influence of each parameter on the classification index can be independently examined. Rock mass block size play the dominant role in determining the rock mass quality. The increase of joint surface roughness (J_R) and

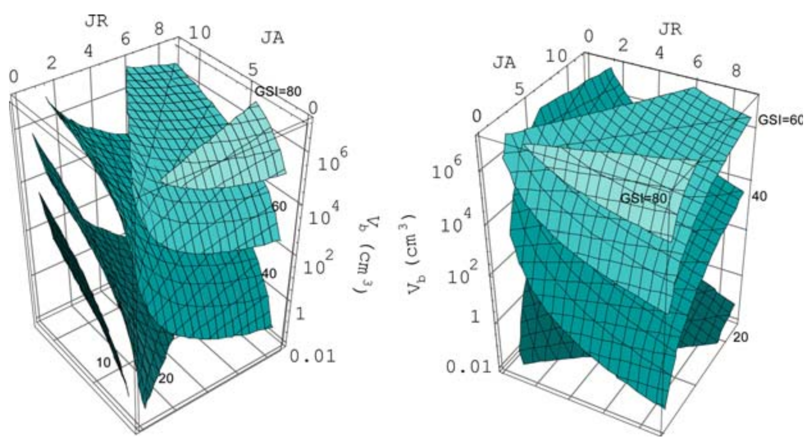

Figure 8. Three-dimensional contours of *GSI* (80, 60, 40, 20, 10). V_b axis is in log scale. Two different views are presented.

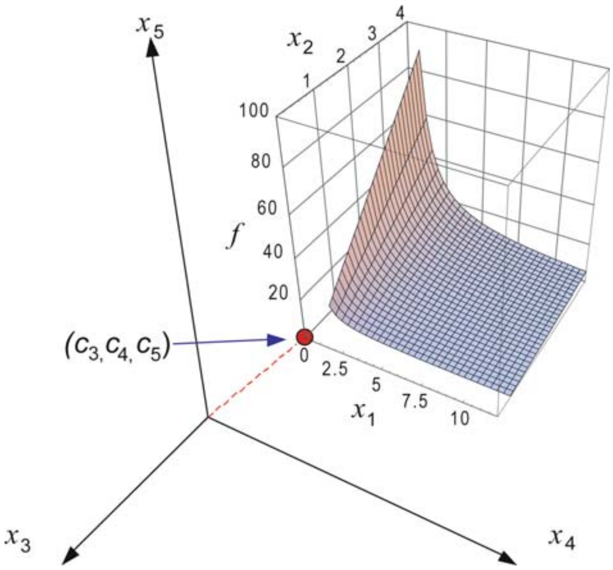

Figure 9. An 5-vision world that encodes a function of five variables as a hierarchy of graphs.

decrease of joint alteration (J_A) result in an increase of the index value. The three-dimensional visualization best fits the system that originally has three independent parameters, such as the *RMi* system. However, when there are more than three parameters and the influence of each parameter on the function needs to be examined in a visual framework, other visualization techniques have to be employed.

5. Visualization in multi-dimensional space

When there are more than three dimensions in a system, it becomes difficult to visualize the function using traditional plots. For example, the modified rock quality index Q' has four independent parameters and in a multi-dimensional visualization, each parameter needs to be considered individually. One method, that is, the worlds within worlds method, is examined in the following discussion for multi-dimensional function/data visualization.

5.1. VISUALIZATION OF THE ROCK MASS CLASSIFICATION SYSTEMS USING WORLDS WITHIN WORLDS METHOD

Beshers and Feiner (1990) proposed the worlds *within worlds*[1] concept, an interactive visualization technique that exploits nested, heterogeneous coordinate systems to map multiple variables onto each of the three spatial dimensions. For a function of five-dimensions,

[1]http://www1.cs.columbia.edu/graphics/projects/AutoVisual/AutoVisual.html#figure_dipstick.

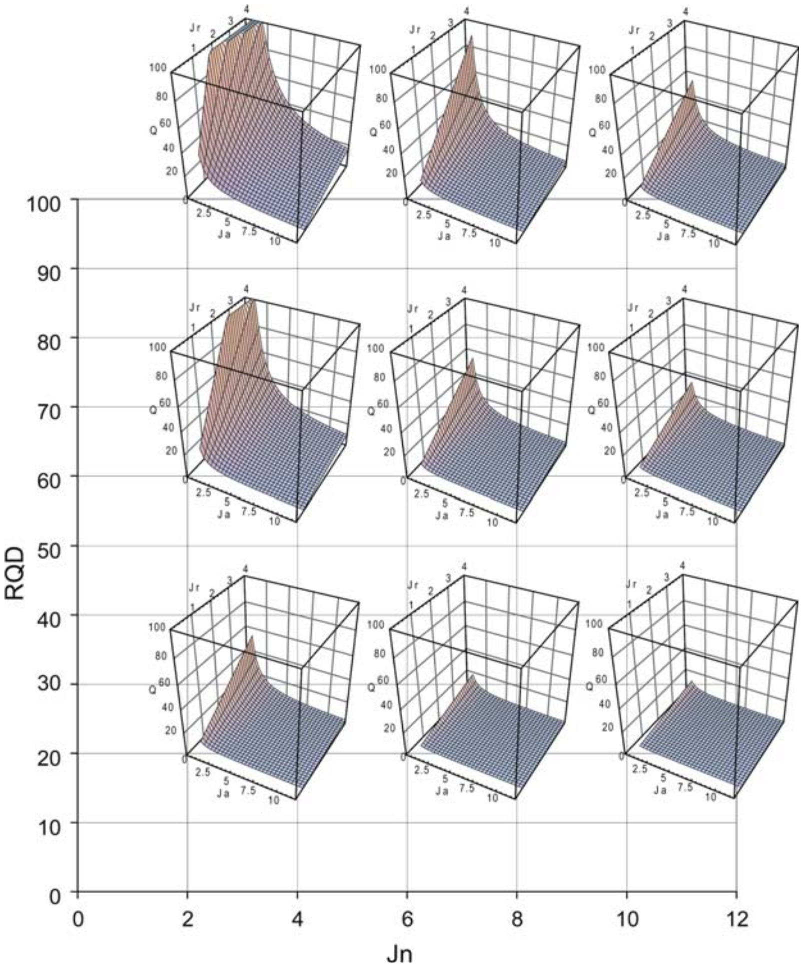

Figure 10. Four-dimensional visualization of the Q' system using the *Worlds within worlds* method.

$$f = f(x_1, x_2, x_3, x_4, x_5) \tag{14}$$

let's first consider constant values for three variables x_3, x_4, x_5, and name them as c_3, c_4, c_5 (Figure 9). This selection results in a new function f':

$$f\prime(x_1, x_2) = f(x_1, x_2, c_3, c_4, c_5) \tag{15}$$

The function f' is easy to graph in three-dimension as a surface plot, with x_1 as the X-axis, x_2 as the Y-axis, and the value of the function as the vertical axis (Z-axis). x_3, x_4, x_5 are plotted in a base figure with a separate set of axes, bound to the X, Y and Z axes. Selecting a point within this larger graph determines the particular values of c_3, c_4, and c_5 used in the smaller graph. The contents of the smaller graph depend on the location of some interactive mark in the larger graph. This dependency is represented explicitly by attaching the origin of the smaller graph (the surface plot, inner world) to the interactive point in the larger graph (outer world). It is obvious that this process can then be repeated by further recursive nesting to visualize *n*-dimensional functions.

Figure 10 presents the Q system visualization using the *worlds within worlds* method. In the outer world, RQD and J_n are designed as the variables in the outer world and in the inner world, J_r and J_a are designed as the variables. Q' values are shown in the small graphs in the vertical axis. Besides using the interactive approach, a series of small graphs are shown in the larger graph to visualize the system. For $J_n = 6$, the influence of RQD on the Q' value can be seen from the series plots shown in the second column. For $RQD = 60$, the influence of J_n on the Q' value can be seen from the series plots shown in the second row. The influence of J_r and J_a on the Q' value can be seen from each individual plot. Using the visualization technique, the influence of constituting parameters (RQD, J_n, J_r and J_a) on Q' can be easily explored and understood. Compared to other methods for multi-dimensional data visualization, the *worlds within worlds* approach is easy to understand and many layers of worlds can be visualized.

6. Conclusions

Abstract rock mass classification systems have been presented by graphs using different visualization techniques. The visualization helps identifying the most important variables in these classification systems, that is, block volume and joint surface condition, for the determination of rock mass properties. From these plots, one can examine the influence of each parameter on the rock mass classification systems and gain valuable insight into these systems.

References

Barton, N. R., Lien, R. and Lunde, J. (1974) Engineering classification of rock masses for the design of tunnel support, *Rock Mech.*, **6**(4), 189–239.

Bieniawski, Z. T. (1973) Engineering classification of jointed rock masses, *Trans. S. Afr. Inst. Civ. Eng.*, **15**, 335–344.

Bieniawski Z. T. (1976) Rock mass classification in rock engineering, in: Proceedings of the Symposium on Exploration for Rock Engineering, Cape Town, Balkema, Vol. 1, pp. 97–106.

Bieniawski, Z. T. (1989), *Engineering rock mass classifications*, Wiley, New York.

Cai, M., Kaiser, P.K., Uno, H., Tasaka, Y. and Minami, M. (2004) Estimation of rock mass strength and deformation modulus of jointed hard rock masses using the GSI system, *Int. J. Rock Mech. Min. Sci.*, **41**(1), 3–19.

Feiner, S. and Beshers, C. (1990) Worlds within worlds: metaphors for exploring n-dimensional virtual worlds, in: Proceedings of the 3rd Annual ACM Symposium on User Interface Software and Technology (UIST'90), Snowbird, UT, USA, pp. 76–83.

Hashash, Y., Wotring, D., Yao, J., Lee, J. and Fu, Q. (2002) Visual framework for development and use of constitutive models, *Int. J. Numer. Anal. Meth. Geomech.*, **26**, 1493–1513.

Hoek, E. and Brown, E. T. (1980) Empirical strength criterion for rock masses, *J. Geotech. Eng. Div, ASCE*, **106**(GT9), 1013–1035.

Hoek, E. and Brown, E. T. (1988) The Hoek–Brown failure criterion – a 1988 update, in Rock engineering for underground excavations, in: Proceedings of the 15th Canadian Rock Mechanical Symposium, Toronto, Canada, University of Toronto, Toronto, pp. 31–38.

Hoek, E. and Brown, E. T. (1997) Practical estimates of rock mass strength, *Int. J. Rock Mech. Min. Sci.*, **34**(8), 1165–1186.

Hoek, E. and Brown, E. T. (1988) The Hoek–Brown failure criterion – a 1988 update, in Rock engineering for underground excavations, in: Proceedings of the 15th Canadian Rock Mechanical Symposium, Toronto, Canada, University of Toronto, Toronto, pp. 31–38.

Hoek, E., Kaiser, P. K. and Bawden, W. F. (1995) *Support of Underground Excavations in Hard Rock*, A.A. Balkema.

Jeremie, B., Scheuermann, G., Frey, J., Yang, Z., Hamann, B., Joy, K. I. and Hagen, H. (2002) Tensor visualizations in computational geomechanics, *Int. J. Numer. Anal. Meth. Geomech.*, **26**, 925–944.

Palmstrøm, A. (1996a) Characterizing rock masses by the RMi for use in practical rock engineering, Part1: The development of the rock mass index (RMi), *Tunnelling and Underground Space Technol*, **11**(2), 175–188.

Palmstrøm, A. (1996b) Characterizing rock masses by the RMi for use in practical rock engineering, Part2: Some practical applications of the rock mass index (RMi), *Tunnelling and Underground Space Technol*, **11**(3), 287–303.

Schroeder, R. (1996) *Possible Worlds: The Social Dynamic of Virtual Reality Technology*, Westview Press. (HarperCollins Publishers, Inc.).

Sen, Z. and Sadagah, B. H. (2003) Modified rock mass classification system by continuous rating, *Eng. Geol.*, **67**(3–4), 269–280.